

## RESEARCH ARTICLE

10.1002/2016JC011723

## Key Points:

- Kallakkadal flooding events along Indian coastline
- Southern Ocean swells
- Cut-off Low and blocking patterns in the Southern Ocean

## Correspondence to:

P. G. Remya,  
remya.pg@incois.gov.in

## Citation:

Remya, P. G., S. Vishnu, B. Praveen Kumar, T. M. Balakrishnan Nair, and B. Rohith (2016), Teleconnection between the North Indian Ocean high swell events and meteorological conditions over the Southern Indian Ocean, *J. Geophys. Res. Oceans*, 121, doi:10.1002/2016JC011723.

Received 13 FEB 2016

Accepted 19 SEP 2016

Accepted article online 21 SEP 2016

## Teleconnection between the North Indian Ocean high swell events and meteorological conditions over the Southern Indian Ocean

P. G. Remya<sup>1</sup>, S. Vishnu<sup>1</sup>, B. Praveen Kumar<sup>1</sup>, T. M. Balakrishnan Nair<sup>1</sup>, and B. Rohith<sup>1</sup>

<sup>1</sup>Indian National Centre for Ocean Information Services, Hyderabad, India

**Abstract** The link between North Indian Ocean (NIO) high swell events and the meteorological conditions over the Southern Indian Ocean (SIO) is explored in this article, using a combination of in situ measurements and model simulations for the year 2005. High waves, without any sign in the local winds, sometimes cause severe flooding events along the south-west coast of India, locally known as the Kallakkadal events and cause major societal problems along the coasts. In situ observations report 10 high swell events in NIO during 2005. Our study confirms that these events are caused by the swells propagating from south of 30°S. In all cases, 3–5 days prior to the high swell events in NIO, we observed a severe low pressure system, called the Cut-Off Low (COL) in the Southern Ocean. These COLs are quasistationary in nature, providing strong ( $\sim 25 \text{ ms}^{-1}$ ) and long duration ( $\sim 3$  days) surface winds over a large fetch; essential conditions for the generation of long-period swells. The intense equator ward winds associated with COLs in the SIO trigger the generation of high waves, which propagate to NIO as swells. Furthermore, these swells cause high wave activity and sometimes Kallakkadal events along the NIO coastal regions, depending on the local topography, angle of incidence, and tidal conditions. Our study shows that such natural hazards along the NIO coasts can be forecasted at least 2 days in advance if the meteorological conditions of the SIO are properly monitored.

### 1. Introduction

Ocean surface waves which are generated by intense storms, travel thousands of kilometers from the generating area across the globe and reach far distant coastal destinations as swells [Barber and Ursell, 1948; Munk et al., 1963; Snodgrass et al., 1966]. These swells play a significant role in the oceanic energy distribution as well as wave climate around the globe [Alves, 2006]. The significant energy carried by the swells impacts on various marine activities and hence swells are treated as inevitable in marine forecasting.

The earliest attempts to study the global nature of swell propagation can be traced back to the works of Barber and Ursell [1948]. Following a spectral analysis of the ocean waves, they identified that the swells that reached Cornwall, England and was generated off Cape Horn at a distance of 11,000 km. Later, seminal papers by Munk and Snodgrass [1957], Munk et al. [1963], and Snodgrass et al. [1966] provided great insights into the swell generation, propagation, and its characteristics. These initial insights were later expanded by numerous studies that looked at the momentum flux at the air-sea interface and lower boundary layer modulations by the swells [Grachev and Fairall, 2001; Grachev et al., 2003; Smedman et al., 2003], modulation of the local sea by the swells [Donelan, 1987; Shyu and Phillips, 1990; Chen and Belcher, 2000], possible role of swells in upper ocean mixing [Babanin, 2006] among many other themes. Recently, there has been growing interest among the wave research community on the propagation and decay of swells which suggests considerable energy dissipation of swells in various oceans [Ardhuin et al., 2009; Collard et al., 2009; Young et al., 2013]. Alves [2006] studied the ocean swell contribution to the global wind wave climate and confirmed that the swells generated in the extra tropical Southern Ocean spread energy throughout the global ocean and are an important component of the global ocean wave climate. All these important studies explored the global nature of swells and provided the necessary impetus for the research on the local impact of swells in creating a modified wave field.

There are many recent studies that identified the Southern Ocean Swells (SOS) as an important and persistent feature of the wave climate year round in the North Indian Ocean (NIO) [Remya et al., 2012; Sabique

*et al.*, 2012; *Nayak et al.*, 2013; *Sandhya et al.*, 2015]. A study by *Nayak et al.* [2013] showed that the low-frequency swells from the Southern Ocean reach the southern tip of Indian mainland in about 4 days without much energy dissipation. Recently *Sandhya et al.* [2015] studied the complex wave field created off the east coast of India during the very severe cyclone Phailin, and attributed it to the interaction of low-frequency swell waves from the Southern Ocean and the cyclone generated waves. All these studies either focus on the complex wave field generated by the swells in the NIO locations or the propagation pattern of the swells from the Southern Ocean into the NIO basins. However, it is also important to understand the processes that generate the swells which eventually propagate into the NIO basins. Such information would be beneficial for the proper forecasting of the high wave events along the NIO coasts as flooding in the coastal regions is a major societal issue affecting millions of people.

The severe coastal flooding events caused by the distant long-period swells is fairly well documented in other basins [*Andrade et al.*, 2013; *Silbey and Cox*, 2015 and references therein], but similar studies are mostly absent in the NIO basins due to lack of proper coastal monitoring and adequate high-quality observations. In the available literature, *Kurian et al.* [2009] has reported a special case of coastal flooding during pre-monsoon (April–May) season by the low-frequency, high-energy SOS on the southwest coast of India. This kind of coastal flooding by SOS is named as Kallakkadal (Kallakkadal is a term used by the fishermen in the state of Kerala in southwest of India to refer to the flash flooding events. In Malayalam (the local language of Kerala, India), *Kallan* means thief and *Kadal* means Sea. In spoken language, these words were combined and pronounced as *Kallakkaadal*, meaning ocean that arrives as a thief. The terminology Kallakkadal was formally approved by the United Nations Educational, Scientific and Cultural Organization (UNESCO) in 2012). It is a flash flooding event without any precursors or any kind of local wind activity to give advance warning to the coastal population. Kallakkadal events are not well documented in scientific literature [*Kurian et al.*, 2009], but attracts lots of media and government attention when the flooding events cause damage to life and property of local population. *Kurian et al.* [2009] postulated the possible reason for the occurrence of Kallakkadal events: the Southern Ocean swells propagate northward, and when it encounters a coastal current directed southward, the swells get amplified through interaction with the current. Due to the increased wave setup, low lying areas on the coast get flooded. When this occurs on spring tide days, flooding will be severe. However, to the best of our knowledge, there is no study that categorically link SOS and Kallakkadal/high wave events in NIO and the causative mechanism of such swell waves in the Southern Ocean.

The prediction of high swell events that cause the Kallakkadal needs close monitoring of the meteorological and oceanographic conditions in the Southern Indian Ocean (SIO), which are marked by intense westerly jet streams circumventing the Earth. Previous studies that report the impact of SOS in the NIO wave conditions, related it to the synoptic storms in the SIO [*Nayak et al.*, 2013; *Sandhya et al.*, 2015]. Apart from the synoptic scale storms, planetary-scale wind patterns associated with the strong meridional gradient of atmospheric pressure fields can also cause meridional undulation of strong westerlies in the Southern Oceans which are called the blocking patterns. These blocking patterns can also provide all the necessary conditions for the generation of swells, which eventually propagate to distant locations. There are basically four different types of blocking patterns, the Cut-Off Low (COL), Blocking high, Rex block, and the Omega block. Among these, the COL systems are very common in SIO [*Fuenzalida et al.*, 2005]. Closed lows in the upper troposphere are called COLs if they are completely detached (“cut off”) from the mean westerly jet streams. A detailed description about the COL is provided in section 2.

The generation of long-period waves like SOS requires intense winds over a longer duration and a large fetch [*Munk et al.*, 1963]. For instance, the generation of waves of period around 18 s with significant energy requires wind speeds of over  $20 \text{ ms}^{-1}$  and a fetch of around 1000 km. COLs are associated with very strong surface winds and ocean turbulence, thus creating high waves [*McInnes and Hubbert*, 2001]. They are slow moving and often stay over the same region for several days making these systems quasistationary [*Bell and Bossart*, 1989], therefore capable of providing the required conditions for the generation of long-period waves. Hence, it is important to explore the connection between the SOS generated by the COLs and the high wave events along the south Indian coasts which, in turn, will help forecasters provide advanced warnings of such events.

Our objectives in this study are twofold. First our goal is to demonstrate the link between Kallakadal events and the SOS. Our second goal is to properly identify the atmospheric-oceanic conditions in the Southern

Ocean that favor the development of SOS that cause flooding events along the Indian coast. Rest of the article is organized as follows: section 2 provides a description of the COLs in the Southern Ocean. Section 3 describes the data used, model details and the methodology followed in this study. Impact of SOS on the NIO high wave events is discussed in section 4 and the relationship of the Southern Ocean meteorological conditions with SOS is explained in section 5. Section 6 contains summary of our results and a discussion on our major findings.

## 2. The Cut-Off Lows in the Southern Indian Ocean

COLs correspond to a closed low geopotential height in the upper troposphere that is completely detached from the basic westerly jets and usually advect equator ward of the midlatitude westerlies [Gimeno *et al.*, 2007a; Nieto *et al.*, 2008]. We follow the methodology of Nieto *et al.* [2008] to detail the various stages of COL development. The schematic of various COL developmental stages are shown in the left plots of Figure 1. The right plots of Figure 1 show the corresponding stages of the evolution of a real COL formed over SIO.

Two initial conditions necessary for the COL development are (i) the presence of an amplifying synoptic scale wave in the upper layers of atmosphere in high latitudes and (ii) a tilt in the vertical axis of the trough of the wave which is in the midlatitudes (see Figure 1a). This causes advection of significant amount of cold air from high latitudes to the midlatitudes. This forms the first stage of a COL development. Second is a tear-off stage in which the geopotential height contour forms an omega shape with a closed low at the center (Figure 1c). At this stage, the trough deepens and gradually gets cut-off from the mean zonal flow. Thus a cold core upper level, low pressure system is formed at the end of the tear-off stage. Third is the cut-off stage that begins when the tear-off is finished (Figure 1e). At this stage, the upper level low become very strong and the wind fields form a well-developed closed circulation. This feature is stronger near 200 hPa and penetrates down to the surface layers. At this stage, COL can be identified from the constant pressure charts as closed contours in the geopotential height with a cold core and cyclonic circulation and moving toward the equator. The final stage refers to the dissipation of COL, which happens either by merging with the mean zonal flow or by drifting over to a warm surface (Figure 1g) in the midlatitudes. The life span of a COL depends on various factors, but the most important is the thermodynamic boundary layer stability below the COL. COLs in the southern hemisphere are mostly found in a nearly zonal belt between subtropics and midlatitudes around the globe [Fuenzalida *et al.*, 2005], and usually lasts for 1–3 days [Reboita *et al.*, 2010].

The different stages of a real COL that developed during 15–17 May 2005 in the SIO are illustrated using the geopotential height, temperature, and winds at 500 hPa (Figure 1, right). On 15 May 12 UTC, along 75°E and in between 40°S and 55°S, the mean westerlies bend toward north forming a trough, which advects cold air from the high latitudes (~65°S–55°S) into the midlatitudes (~45°S–40°S). In the tear-off stage, a closed cyclonic circulation pattern formed along 40°S–45°S, 80°E (Figure 1d), which then grew into a strong low geopotential center (Figure 1f). Mean westerlies are present south of the geopotential center, but north of it, very strong south-westerlies exist on the left and north-westerlies on the right. This fully developed COL system (around 45°S, 100°E), was very slow moving, thus stagnated the weather patterns over the SIO for around 2 days until 16 May 18 UTC. The system finally weakened on 17 May 18 UTC.

## 3. Data, Model Description, and Methodology

### 3.1. Data

A combination of in situ observations and numerical model simulations are used in this study. In situ wave observations are from four shallow water moored buoys (SW3, SW4, SW5, and SW6) and one deep sea moored buoy (DS5) around the Indian coasts and Bay of Bengal (BoB), respectively ([www.incois.gov.in/portal/datainfo/mb.jsp](http://www.incois.gov.in/portal/datainfo/mb.jsp)). The buoy locations are marked in Figure 2. The shallow water buoys SW4 (12.94°N, 74.72°E; off Mangalore,) and SW3 (15.4°N, 73.75°E; off Goa) are located along the south-west coast whereas SW5 (8.7°N, 78.23°E; off Tuticorin) and SW6 (15.4°N, 73.75°E; off Ennore port) are located along the south-east coast of India. Wave spectra data are available only from the DS5 deep sea mooring (14°N, 83.27°E; off Visakhapatnam in the BoB). Our analysis period is restricted to the year 2005 due to two reasons: (1) The strongest Kallakkadal event was reported during 17–21 May 2005, and (2) adequate observations are available only for 2005. The shallow water observations are continuously available only from March through May of 2005, whereas the deep sea mooring observations are available continuously for whole of 2005. We use

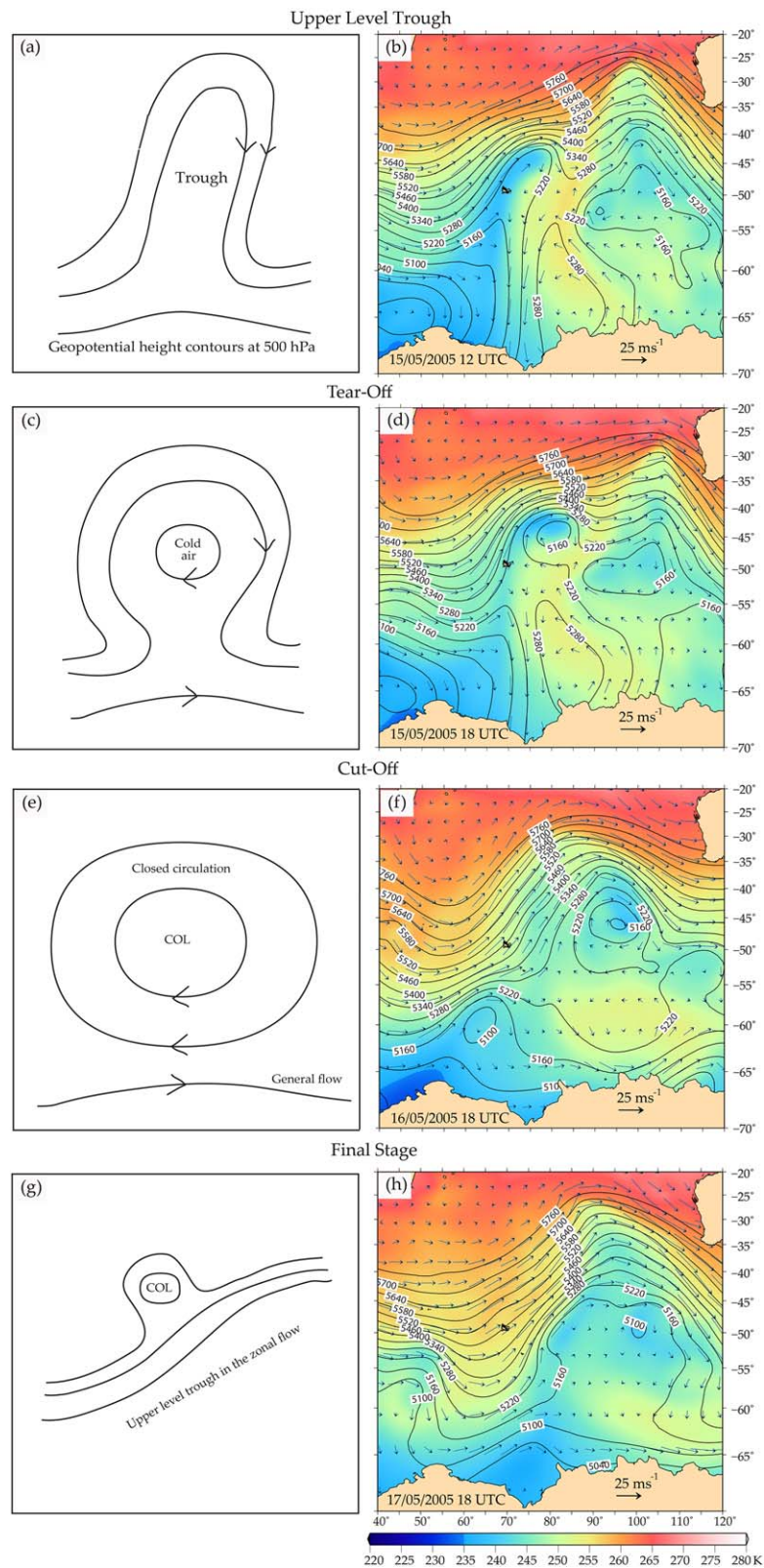


**Figure 1.** (left) Schematic of the various stages of Cut-Off Low development over the southern hemisphere. (right) A real case of Cut-Off Low development over the Southern Indian Ocean during 15–17 May 2005. Temperature (shaded; K), geopotential height (contour; gpm) and winds (vectors; m/s) are used to depict the different stages of Cut-Off Low.

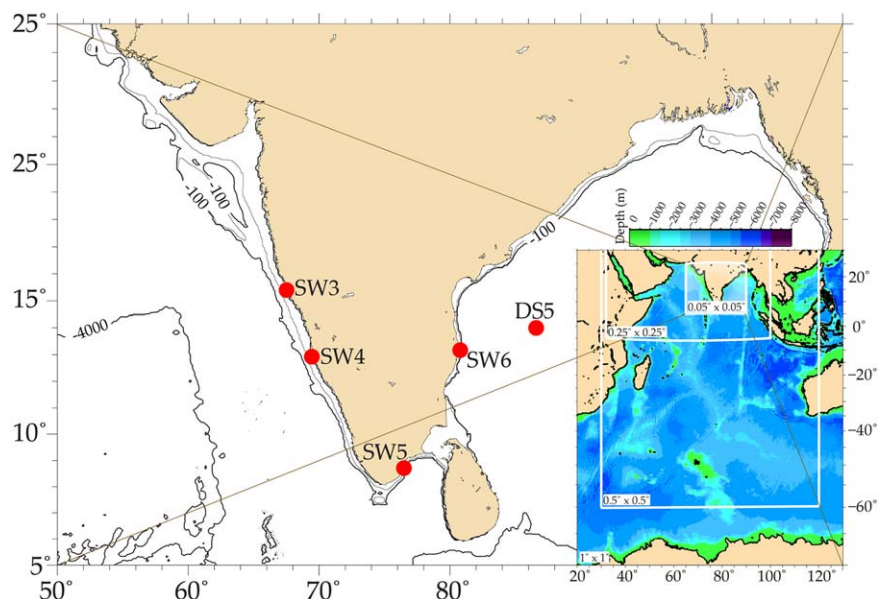


**Figure 2.** Locations of in situ buoy observations (red circles) used in this study. The east coast buoys are SW4—off Mangalore and SW3—off Goa and the west coast buoys are SW5—off Tuticorin, and SW6—off Ennore port. The deep sea mooring DS5 is off Visakhapatnam in the Bay of Bengal. Figure in the inset shows the model domain for the study, and model grids spacing used are shown in the inset figure.

observations of significant wave height ( $H_s$ ), swell height ( $H_{ss}$ ), mean wave period ( $T_m$ ), and peak wave period ( $T_p$ ) from the buoys for the wave analysis.

We also used sea level pressure, geopotential height, and air temperature, both at 500 and 300 hPa pressure levels ( $0.75^\circ$  spatial resolution, 6 hourly) from the Interim analysis of European Centre for Medium-Range Weather Forecasting (ECMWF), ERA Interim [Dee *et al.*, 2011] for the identification of COLs. French Research Institute for Exploitation of the Sea (IFREMER) blended wind fields ( $0.25^\circ$  spatial resolution, 6 hourly, <ftp://ftp.ifremer.fr/ifremer/cersat/products/gridded/mwf-blended/data>) [Bentamy *et al.*, 2007] and QuikSCAT daily data (ascending and descending passes,  $0.25^\circ$  spatial resolution, [www.remss.com](http://www.remss.com)) are also used for the analysis.

### 3.2. Model Description

Model wave fields for the study are generated using WAVEWATCH III (WW3), version 4.18 [Tolman and the WAVEWATCH III<sup>®</sup> Development Group, 2014], using the new parameterization scheme ST4 by Ardhuin *et al.* [2010]. Simulations were performed using a four grid mosaic WW3 with a global grid ( $1^\circ$  spatial resolution), multiple regional grids (Indian Ocean at  $0.5^\circ$  spatial resolution and NIO at  $0.25^\circ$  spatial resolution) and a coastal grid ( $0.05^\circ$  spatial resolution) for the Indian Ocean region (see inset of Figure 2) and forcing with IFREMER blended wind fields [Bentamy *et al.*, 2007]. We have used a spectral grid consisting of 29 frequencies (initial frequency is 0.035 Hz with an increment factor 1.1) and 36 directions.

Simulated wave fields for the study are generated in two separate wave model runs done for the period January–December, 2005. In the control run, we use active wind forcing at all the grid points in the model domain. Whereas in the experimental run setup, we force the model with active winds only in the SIO ( $60^\circ\text{S}$ – $30^\circ\text{S}$ ;  $40^\circ\text{E}$ – $100^\circ\text{E}$ ). Thus comparing the control run and experimental run would identify the contribution of SOS in the total wave field observed in the NIO. The model error statistics at the selected buoy locations are provided in the Appendix A.

### 3.3. Identification of Swell Events

The characteristics of the waves associated with the Kallakkadal events are long-period waves ( $\sim 15$  s) with moderate  $H_s$  (1.25–2.5 m) and have durations of a few days [Kurian *et al.*, 2009]. To identify the high swell events, we filtered all the long-period waves ( $\geq 15$  s) that are having a swell wave height of at least 0.5 m and lasting more than 12 h in the buoy measurements. For separating sea and swells from the wave

spectrum data, measurements between 0.04 and 0.1 Hz are considered to be low-frequency (swell) components and 0.1–0.5 Hz are taken as high-frequency (sea) components.

### 3.4. Identification of Cut-Off Lows

COLs are described using the geopotential height and temperature fields at 500 and 300 hPa levels over the SIO domain (60°S–30°S and 40°E–100°E). The COLs are identified when they are having (i) a closed low geopotential height in the upper air (ii) a cold temperature core, and (iii) cut-off circulation from westerlies. Sea level pressure data are used to identify the COL extension to the surface. Duration and size of the COLs are found based on the criteria of *Singleton and Reason* [2007], using the geopotential height at 300 hPa. The duration of the COL is defined as the time for which at least one closed geopotential height at the 300 hPa contour is within the SIO domain. The size of the COL is defined as the latitudinal width of the outer closed contour of the system.

Persistence of the COLs over the path of the fast moving jet streams block the normal course of the jets as the COLs move very slowly, creating a blocking pattern. An intense COL system can effectively block the jet stream mean flow, thus leading to the stagnation of weather patterns and strong surface winds over a large area. Thus the Blocking Intensity (BI) is an important metric that defines the strength of the COL to produce the long-period swells [*Lupo and Smith* 1995a; *Wiedenmann et al.*, 2002]. Following *Wiedenmann et al.*, [2002], expression for the BI in order to estimate the intensity of COL can be written as,

$$BI = 100.0 \left[ \frac{RC}{MZ} - 1 \right]$$

where MZ is the minimum 500 hPa geopotential height in the closed COL region or on a line associated with the trough axis, RC is the “mean contour” estimated across the area encompassed by the upstream and downstream troughs at the same latitude as the block center. RC is computed as follows,

$$RC = \frac{\left( \frac{Z_u + MZ}{2} \right) + \left( \frac{Z_d + MZ}{2} \right)}{2}$$

where  $Z_u$  ( $Z_d$ ) represents the highest geopotential height value in the trough axis upstream (downstream) of the block center in the same latitude. Based on this method, the intensity of blocking events in the southern hemisphere is categorized as, weak ( $BI < 2.0$ ), moderate ( $2.0 < BI < 3.6$ ), and strong ( $BI > 3.6$ ).

## 4. High Swell Events in the North Indian Ocean During 2005

Major high wave events, with instances of Kallakkadal flooding along the south-west coast of India are reported in the pre-monsoon season (March–May) of 2005 and hence in the coming sections we focus on that season unless otherwise specified. The high swell events, (criteria as described in section 3.3) recorded by the buoys during the pre-monsoon season of 2005 are shown in Figure 3.

Filtered data shows six major events of high swells in the west coast of India (SW4 and SW3 – one event each in March and April and four events in May. See the gray shading in Figures 3a and 3b). Less number of swell events are observed in the east coast of India (SW5 – four events and SW6 – two events, Figures 3c and 3d). The wave spectra of the deep water buoy DS5 also shows five major events except the one in March (Figure 3e). The coastal flooding due to high waves is mainly reported along the south west coast of India [*Kurian et al.*, 2009] and hence the SW4 buoy is considered as our reference for the analysis in the pre-monsoon period. In the following sections, we focus on the 17–21 May 2005 period since all the buoys picked that strongest wave event, and also it caused Kallakkadal flooding event along the south-west coast of India.

Waves generated in the fetch area undergo nonlinear interactions and leave the fetch as swells. Long-period swells coming out from the fetch travel fast and are called the forerunners, followed by short-period swells. Hence swells observed at a distant location will be the long-period swells first and then the short-period ones. Wave parameters,  $H_s$ ,  $T_p$ , and  $H_{ss}$  observed at the south-west coast of India (SW4) are shown in Figure 4. At SW4 location,  $H_s$  showed a gradual increase (0.7–1.2 m), as a result of the corresponding increase in the  $H_{ss}$  as seen from Figure 4. Long-period swells of  $\sim 20$  s were observed on 17 May, followed by short-period waves. This indicates that swells with a band of frequencies are arriving at the location on

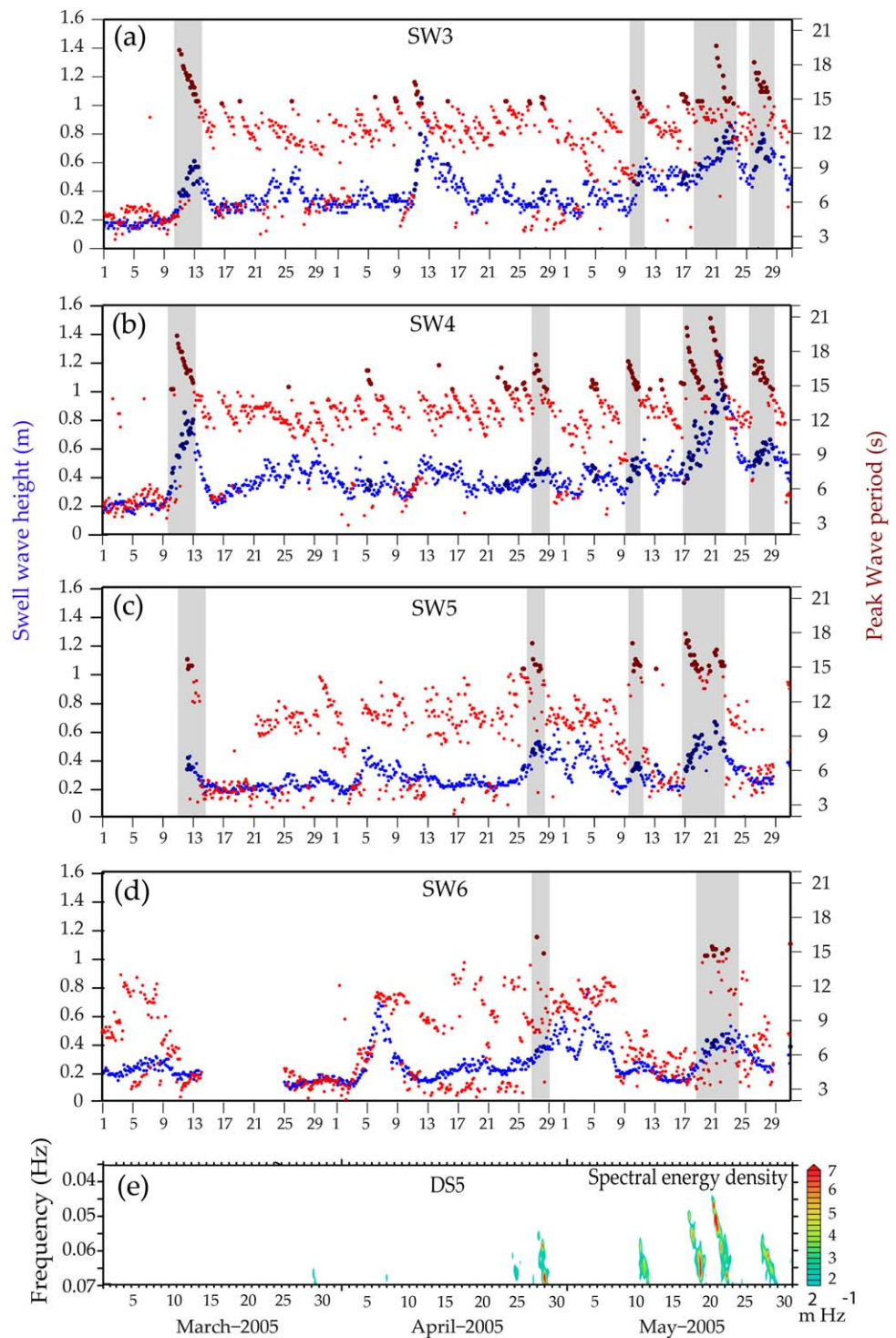


**Figure 3.** Time series plots of swell wave height (blue) and peak wave period (red) for the shallow water buoys during March–May 2005. The gray-shaded portions represent major long-period swell occurrence. (e) Evolution of wave energy density spectrum ( $\text{m}^2\text{Hz}^{-1}$ ) at the deep sea mooring location (DS5) during the same period.

17 May and caused an increase in the Hss. The wave period gradually decreased and remained nearly constant ( $\sim 14\text{s}$ ) till in the early hours of 20 May. Then a new band of swell waves with a period  $\sim 20\text{s}$  started arriving at the location. This is an indication of another swell system from a different origin reaching the buoy location. In the second case too, the major contribution to the Hs was from the swells. Thus the high

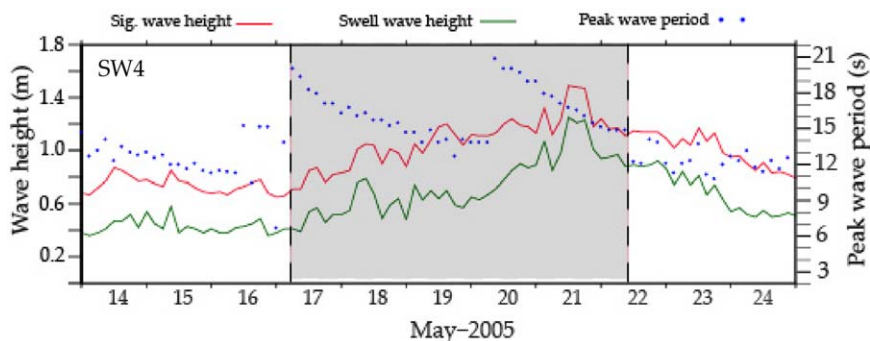


**Figure 4.** Time series plot of significant wave height (red), peak wave period (dotted blue), and swell wave height (green) from the SW4 buoy, along the south west coast of India. Shaded portion represents the strong swell event during 17–21 May 2005.

wave activity observed during 17–20 May was, in fact, caused by swells and not by local winds. Our analysis further showed that there were two sets of swells with different origin that reached the buoy location, though they might be generated from the same region.

The wave spectral energy observed at the deep sea mooring DS5 is shown in Figure 5a that clearly shows two peaks in energy density associated with the high swell events observed at the shallow water mooring locations. In the control run that we conducted using WW3 with active winds at all the grid points, the spectral peaks are well reproduced as compared to observations (see Figure 5b), though with an overestimation of amplitude. Our earlier analysis (Figure 4) suggests that the peaks in the wave field observed at the mooring locations are due to the arrival of low-frequency swells, but the genesis area of the swells is unknown. Taking a clue from many past studies that suggest that SOS reaches the NIO basins [Remya *et al.*, 2012; Nayak *et al.*, 2013], we have done a model experimental run in which we applied active winds only in the Southern Ocean (40°E–100°E and 60°S–30°S). The spectral data from the experimental run are shown in Figure 5c. Nearly one to one comparison of Figures 5b and 5c suggests that winds north of the Southern Ocean limits do not have any significant contribution on the swells observed at the NIO buoy locations. This confirms that the two swell events, which caused high wave activity and a Kallakkadal event during 17 May on the south-west coast of India, are in fact coming from the Southern Ocean, south of 30°S.

Now referring back to Figure 3, SW6 shallow water mooring captured least number of high swell events compared to other locations. The reason for that might be that the geological feature referred to as Adam’s bridge or Ram Sethu (located between Sri Lanka and India) could be playing a critical role in blocking the high swells from the Southern Ocean that hit the southern tip off India, from entering in to the south-east coast of India. Also, the SW6 buoy is located in the shadow region of Sri Lanka which prevents the swells

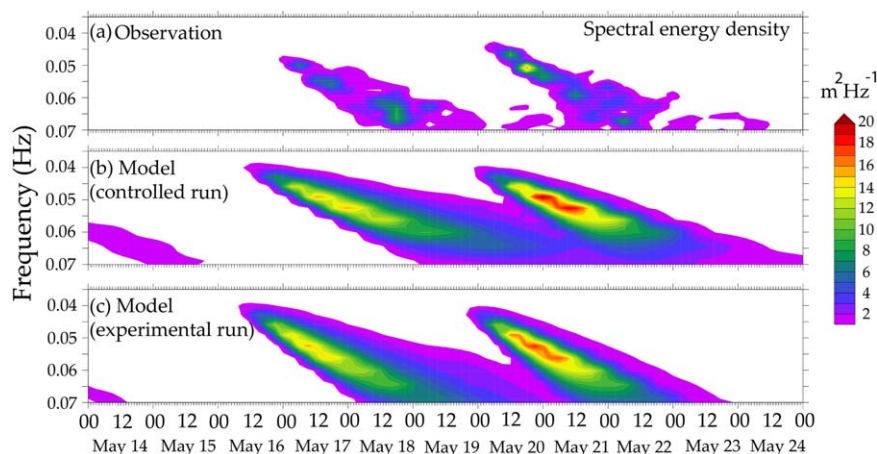


**Figure 5.** The evolution of wave energy density spectrum in (a) Observation (b) model control run, and (c) model sensitivity experiment during 14–24 May 2005 at the deep water mooring location DS5.

from reaching the buoy location. Thus the presence of Adam's bridge or Ram Sethu and Sri Lanka act as a natural damping mechanism to arrest the SOS from causing high wave activity along the south-east coast of India.

In this section, we analyzed the buoy wave parameters to trace the cause of high wave activity observed in the NIO basins. Our analysis suggests that the increase in the significant wave height at the buoy locations are in fact contributed by swells from the Southern Ocean, and not by local waves. In the coming sections, we analyze the ocean-atmosphere conditions in the SIO that generate the swells.

## 5. Southern Indian Ocean Meteorological Conditions Prior to the NIO High Wave Events

A detailed analysis of the meteorological conditions over the SIO from where the low-frequency swells are generated is provided in this section. Initially, we focus on the case study of the strongest Kallakadal event, 17–21 May 2005. Then, we extend our analysis for the cases of other high swell events observed in 2005 to confirm our results from the case study.

### 5.1. Case Study of the May 2005 Flooding Events

Swell waves from the Southern Ocean [70°S–40°S and 40°E–110°E] reach the southern tip of India in about 4 days [Nayak *et al.*, 2013]. To establish the link between the high swells at NIO and their origins in the Southern Ocean, an analysis of sea level pressure, geopotential height at 500 hPa, and surface winds for an early period 12–17 May, 2005 has been carried out.

The geopotential height at 500 hPa over SIO is monitored for the identification of the COL events in the upper atmosphere whereas sea level pressure and surface winds are analyzed to identify the footprint of the COLs at the sea surface (Figure 6). Formation of a trough was clear at around 65°E, 50°S on 11 May 18 UTC with the 5160 gpm contour extending to about 50°S (Figure 6a). This shows the initial stages of the development of a COL system. A closed circulation was formed by 00 UTC of 12 May both at the surface and at 500 hPa, which becomes prominent on 12 May 18 UTC as evident from the closed geopotential contours (Figure 6b). This feature continued to strengthen and reached its peak on 14 May 00 UTC (Figure 6c). It is noted that the geopotential height at 500 hPa and sea level pressure covary and show strong spatial correspondence (Figures 6a–6c). Figure 7a shows the observed strong equator ward surface winds from QuikSCAT, which verify the strong winds associated with COL development. The COL thus developed was slow moving and during the 36 h period from 00 UTC of 13 May to 12 UTC of 14 May, COL deepened, tightening the surface pressure gradient in the north west-south east direction. This resulted in a rapid increase of south-westerly surface winds over the north-western side of the pressure center, as seen during these hours (Figures 6b–6c). The COL had a strong meridional extent of winds, from 60°S to 30°S, with maximum winds of up to 28 ms<sup>-1</sup>. A large area of  $\sim 3 \times 10^6$  km<sup>2</sup> ( $\sim 30^\circ$  in meridional and  $\sim 10^\circ$  in zonal extent) experienced persistently strong winds of  $\sim 25$  ms<sup>-1</sup> in the north-west quadrant for over a day (Figures 6c and 7a). BI index shows that the intensity of the COL was from moderate (2.43 on 12 May) to strong (4.66 on 14 May). The system was at its peak intensity on 14 May and then started weakening.

The formation of the first COL was immediately followed by another COL, which started developing over the same region on 15 May and reached its peak intensity during the late hours of 16 May, before weakening on 17 May (Figures 6d–6f). Figure 6d shows the development of the trough on 15 May 12 UTC over the same region as the first one which is then formed an omega shape on 18 UTC of the same day (Figure 6e). On 16 May 18 UTC, the COL reached its peak intensity (BI = 4.17) showing a strong northward component of wind with a speed of  $\sim 28$  ms<sup>-1</sup> in the north-west of the pressure center (Figure 6f). The strong surface wind fields observed in the QuikSCAT scatterometer during 17 May at 00 UTC confirm the same (Figure 7b). The system remained quasistationary in the place till 17 May and started weakening on the late hours of the same day. BI index shows that the intensity of the second COL was from moderate (2.91 on 15 May) to strong (4.17 on 16 May).

The two COL systems stayed quasistationary for 3 days, providing conducive conditions (ample duration, fetch, and wind speed) for the high waves to be generated. We used wave model simulations to study the wave characteristics and its propagation patterns between the storm source and swell landfall. In the first case, the COL duration was about 3 days and strong south-westerly surface winds of more than 25 ms<sup>-1</sup>

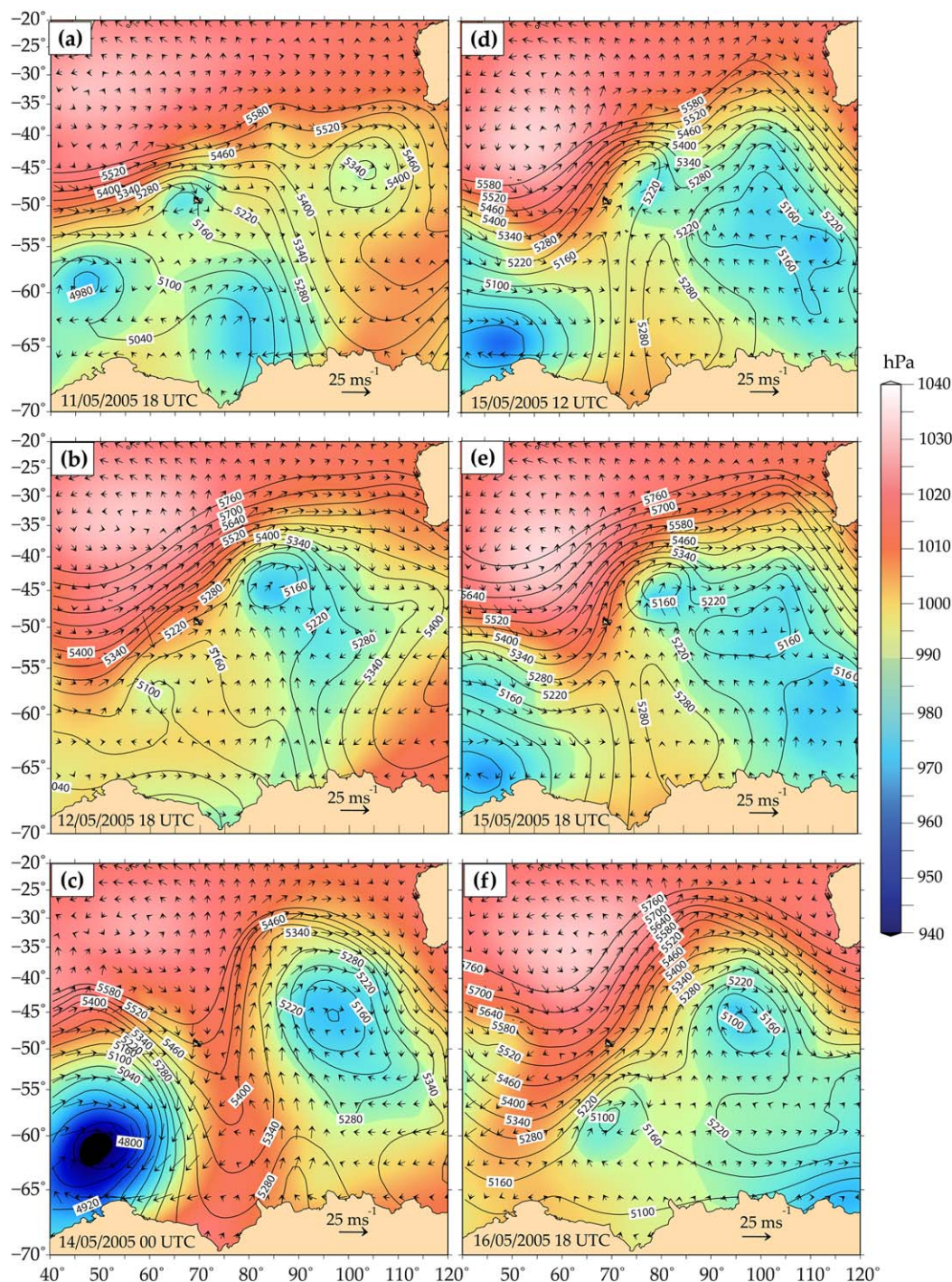


**Figure 6.** Maps showing the evolution of Cut-Off Lows during 12–17 May 2005 in the Southern Indian Ocean. Here, geopotential height (gpm) at 500 hpa is in contours, sea level pressure (hPa) is shaded, and surface winds (m/s) are shown as vectors.

persisted during the period. These strong and persistent winds generated high waves at the COL active region and the maximum  $H_s$  generated was around 13 m (Figure 8a). The strong south south-westerly surface wind fields associated with the COL, generated waves that propagate towards north north-east into the NIO in a band of frequencies with a peak wave period of around 20 s (Figures 8a and 8b). The north ward propagation of primary swells, which is the first dominant swell [Tracy *et al.*, 2007], from the source area (region of COL) is shown in Figures 9a and 9b. High swell waves of the order of 6 m flooded the

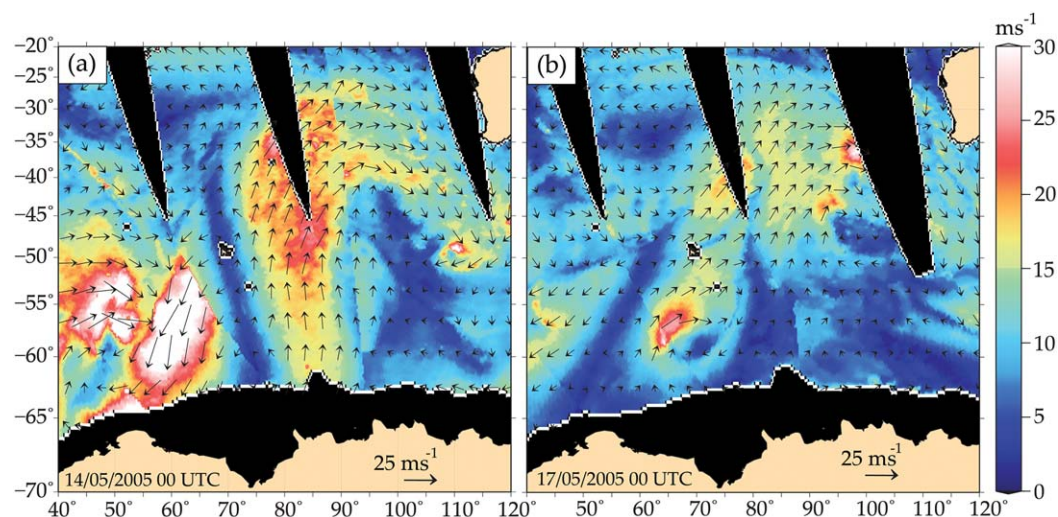


**Figure 7.** Surface wind fields from QuikSCAT scatterometer during 14 and 17 May 2005. Shade represents the magnitude of the surface winds and arrows show its direction.

western Australian coast, which is the closest land mass from the swell generation area, causing severe life and property damages [Jones *et al.*, 2005]. During the propagation toward NIO, high waves hit the coasts of Sumatra and Maldives. Then finally the swell waves hit on south west coast of India on 17 May. This was the first swell system which was observed at the south-west coast on 17 May 2005 and observed in the mooring locations (see Figures 4 and 5). Further, the high swells hit Andaman Nicobar islands, north east coasts of India (Orissa, West Bengal), coasts of Bangladesh, and Myanmar.  $H_s$  range in the BoB was around 2–3 m during 17–19 May period. When the waves were generated in the Southern Ocean, the energy was focused towards north-east of NIO and hence the energy of the waves in the eastern Arabian Sea (AS) was less than half of the energy ( $H_s \approx 1$ –1.5 m) in the BoB. Analysis of the peak wave period shows that even though the impact was less in the eastern AS, the swell waves reached up to the coast of Oman (Figure 8). Model results indicate that traces of this swell energy might have entered in the Persian Gulf as well.

Observations show that initially the swell waves with a period of 20 s hit off Mangalore, west coast of India (SW4 buoy) on 17 May 06 UTC (Figure 4). The group velocity of the wave can be calculated as,  $C_g = g/4\pi f$ , which is  $15.6 \text{ ms}^{-1}$ . The source area, as seen in the model, is approximately 5700 km away from the buoy location. If a wave travels with a group velocity of  $15.6 \text{ ms}^{-1}$ , then it takes approximately 4 days to reach the buoy location. In short, a swell wave which originates in the Southern Ocean on 13 May would hit the south west coast of India after 4 days on 17 May. Thus the cause Kallakkadal event reported on 17 May 2005 along south-west coast of India can be traced back to the swells propagated from the Southern Ocean,  $\sim 5700$  km south of the buoy location, developed as a result of a strong COL system.

The development of another COL system at about the same location on 15 May 2005 triggered the propagation of a band of frequencies towards NIO before the complete dissipation of the first swell system. In addition, the aggravated sea state created by the first COL system might have made the wave development more effective in the second event. Same as during the first COL, strong northward winds were associated with the second COL and caused the wave propagation towards NIO in the north-north east direction (Figure 8c). The maximum  $H_s$  at the origin was around 16 m. The high waves first affected the western Australian coastal regions, then Sumatra, Maldives, and continued its propagation toward NIO. The waves hit the southwest coast of India on 19 May and were the source of second swell system observed in the buoy measurements (Figure 4). The wave height in AS and BoB are in the range of 1.5–2 and 2–3 m, respectively. As in the earlier case, the high swells affected Andaman Nicobar islands, other Indian coastal regions, coasts of Bangladesh, Myanmar, and Oman.

From the above described sequence of events, it is clear that the two consecutive strong SIO COLs ( $BI > 3.6$ ) during the period 12–17 May 2005, generated the high energy, low-frequency swells which caused coastal flooding in the south west coast of India during 17–21 May. The long-period ( $\sim 20$  s) forerunners hit the

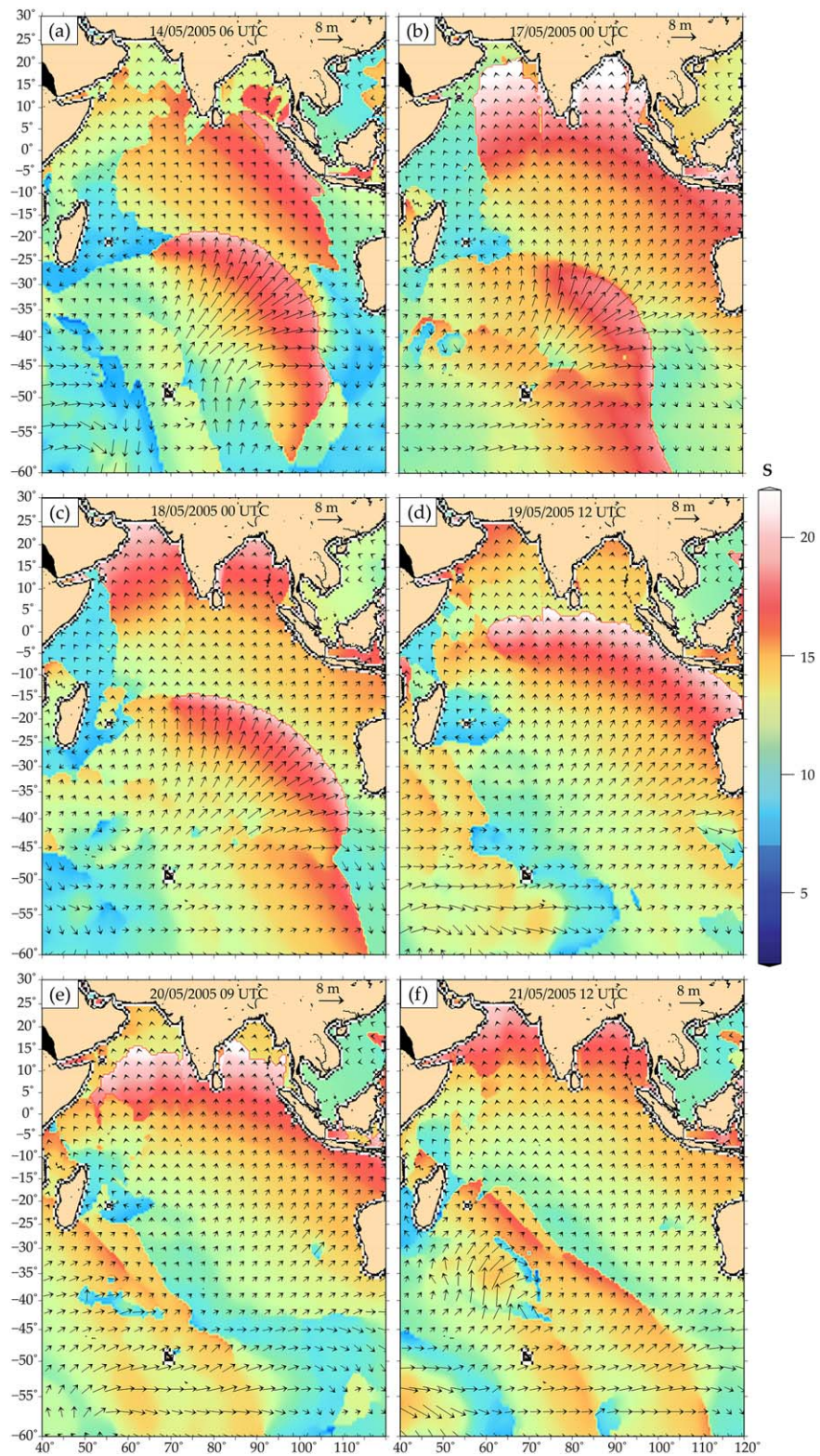


**Figure 8.** Maps of peak wave period (shaded) and wave height (vectors) showing the wave propagation in the Indian Ocean during 14–21 May 2005.

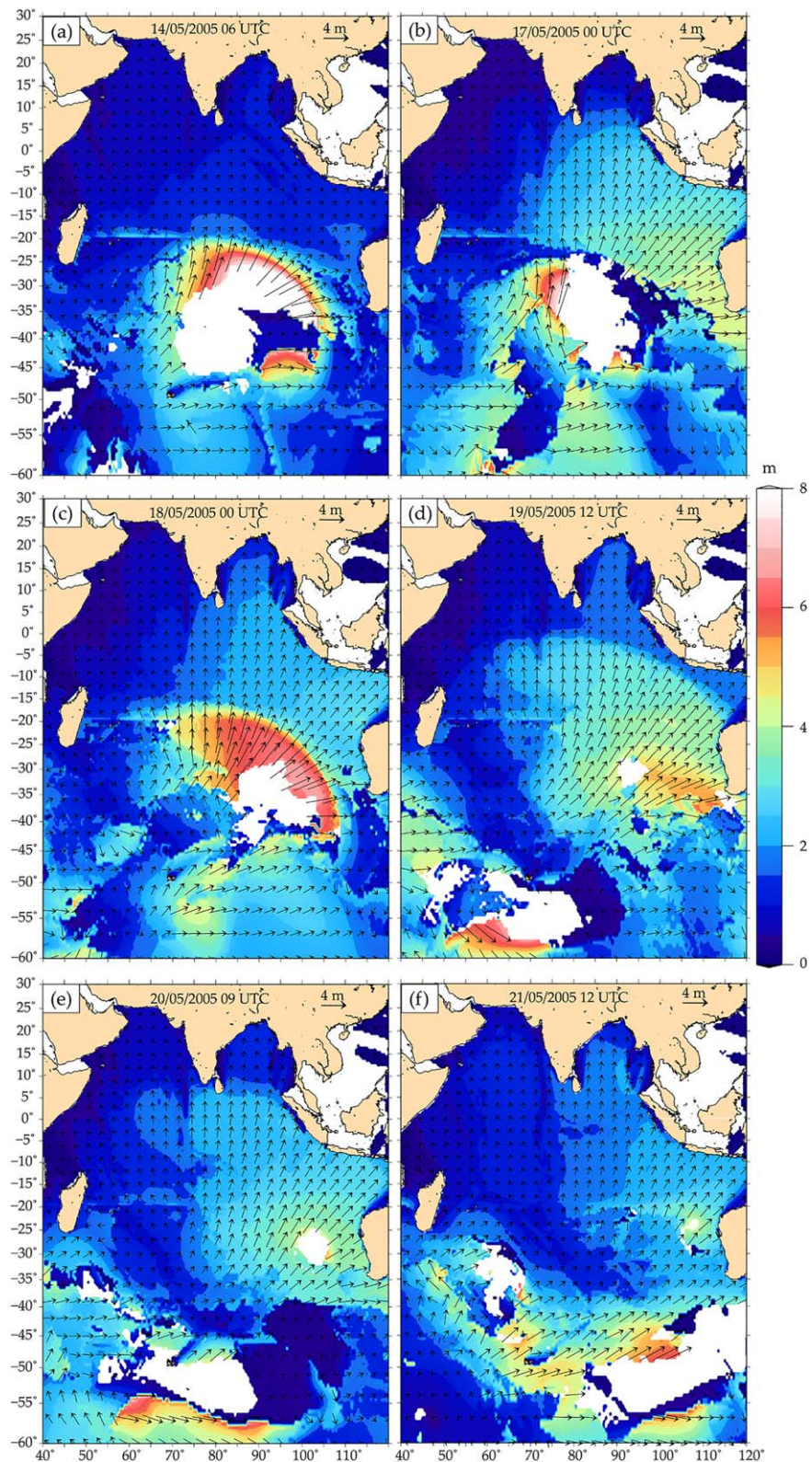


**Figure 9.** Maps of primary swell (arrows show the direction) propagation in the Indian ocean during 14–21 May 2005. Here, white shade shows wind sea domination.

**Table 1.** Characteristic Details of South Indian Ocean Cut-Off Lows and the Associated Swell Events During the Pre-Monsoon Period Recorded at the SW4 Buoy

Date	Southern Ocean COL					Swell Events Off South West Coast of India			
	Peak Intensity Location	BI	Duration (days)	Width (km)	U10 (m/s)	Date	Hs (m)	Tp (s)	Hss (m)
07-03-2005	42.85 77.62E	3.96	2	1890	18	2005-03-10	1.04	19.34	0.64
21-04-2005	47.25 88.88E	4.25	1.25	880	28	2005-04-27	0.66	17.695	0.43
07-05-2005	39.45 79.88E	3.51	6.25	2090	21	2005-05-09	0.85	17.11	0.47
14-05-2005	36S 90.00E	4.66	3.25	2420	28	2005-05-17	0.97	20.03	0.6
16-05-2005	38.25 90.00E	4.17	3	1210	34	2005-05-20	1.22	20.86	0.94
22-05-2005	36S 68.62E	3.24	2.5	1760	26	2005-05-27	0.85	17.34	0.57

coast first, followed by a band of swell waves with decreasing period and this continued for at least 2 days in each case. The wave length of the waves derived from the model in the southwest coast of India (SW4 buoy location) was in the range 220–260 m (not shown). Due to the shoaling in the coastal areas, these waves can cause increased wave setup in the breaking zones and a high tide in the region intensifies the inundation. This can be the possible reason for the coastal flooding during such swell events in the low lying NIO coastal areas. Flooding is mostly reported along the south west coast of India [Kurian *et al.*, 2009] during this period. Narrowness on the continental shelf of south west coast of India and the near perpendicular impact of swells on the shelf enhance the increase of wave height compared to the other coasts.

### 5.2. Other NIO Swell Events in 2005

Analysis of the meteorological conditions over the SIO prior to the other pre-monsoon swell events further support the relation between SIO COLs and the swell events in the NIO. We follow the same methodology as done before to relate the generation mechanism of swell events to SIO COLs and the details of the characteristics of all the pre-monsoon swell events and the corresponding SIO COLs are given in Table 1.

COL characteristics in the SIO prior to the remaining four pre-monsoon swell events are shown in Figure 10. These swell events observed at the mooring location (SW4; Figure 3) also show a clear connection with the moderate to strong category SIO COLs (Table 1 and Figure 10) developed 3–5 days before. The COL that was developed on 7 May 2005 persisted in the region for around 6 days and created long swells over the period of time. Among the pre-monsoon COLs, 12–17 May events were in the stronger category and had duration around 3 days (Table 1). The COL detected on 21 April also comes under strong category (BI > 3.6) but its location was far south and had a short duration (less than one and half days). Also, the swell propagation in this case was in the east north-east direction i.e., more toward southern Australia (Figure 10f), rather than toward north. In all cases, the swells from the Southern Ocean took 3–5 days to reach the NIO basins (see Table 1).

To generalize our inferences so far, all the high period swell events reported for 2005 are also analyzed using the wave spectra data from the DS5 location (Figure 11). Occurrence of high swell events is limited mostly during the March–November period (Figure 11). High waves and Kallakkadal events are also sometimes reported in the post-monsoon season [Kurian *et al.*, 2009]. The details of the characteristics of all the swell events reported from the DS5 location and the corresponding SIO COLs are given in Table 2. Inferences obtained for the pre-monsoon swell events from the SW4 buoy data are consistent with the observations for the same period from the DS5 location (Table 2). Moderate to strong COLs are also seen in the monsoon and post-monsoon cases and the swell propagation from the area is confirmed using the modelled wave parameters. The COLs are under moderate category except the June case. In all cases, the swells from the Southern Ocean took 3–5 days to reach the NIO basins. Thus, the association of swell events causing high wave activity in the NIO and the COLs in the SIO is established in all the cases of high wave events observed in the NIO buoys during 2005 (Tables 1 and 2).

From Tables 1 and 2, it is shown that the duration of COLs in most of the cases are more than 2 days and the surface wind speed in excess of 20 ms<sup>-1</sup>. Additionally, vast swathes of land free SIO provide enough fetch to support the wave growth. These three factors, i.e., long duration, high wind speeds, and large fetch, are thus responsible for the generation of high waves in SIO and spread energy in the entire Indian Ocean through swell propagation. The locations and intensity of COLs given in the tables manifest that a strong

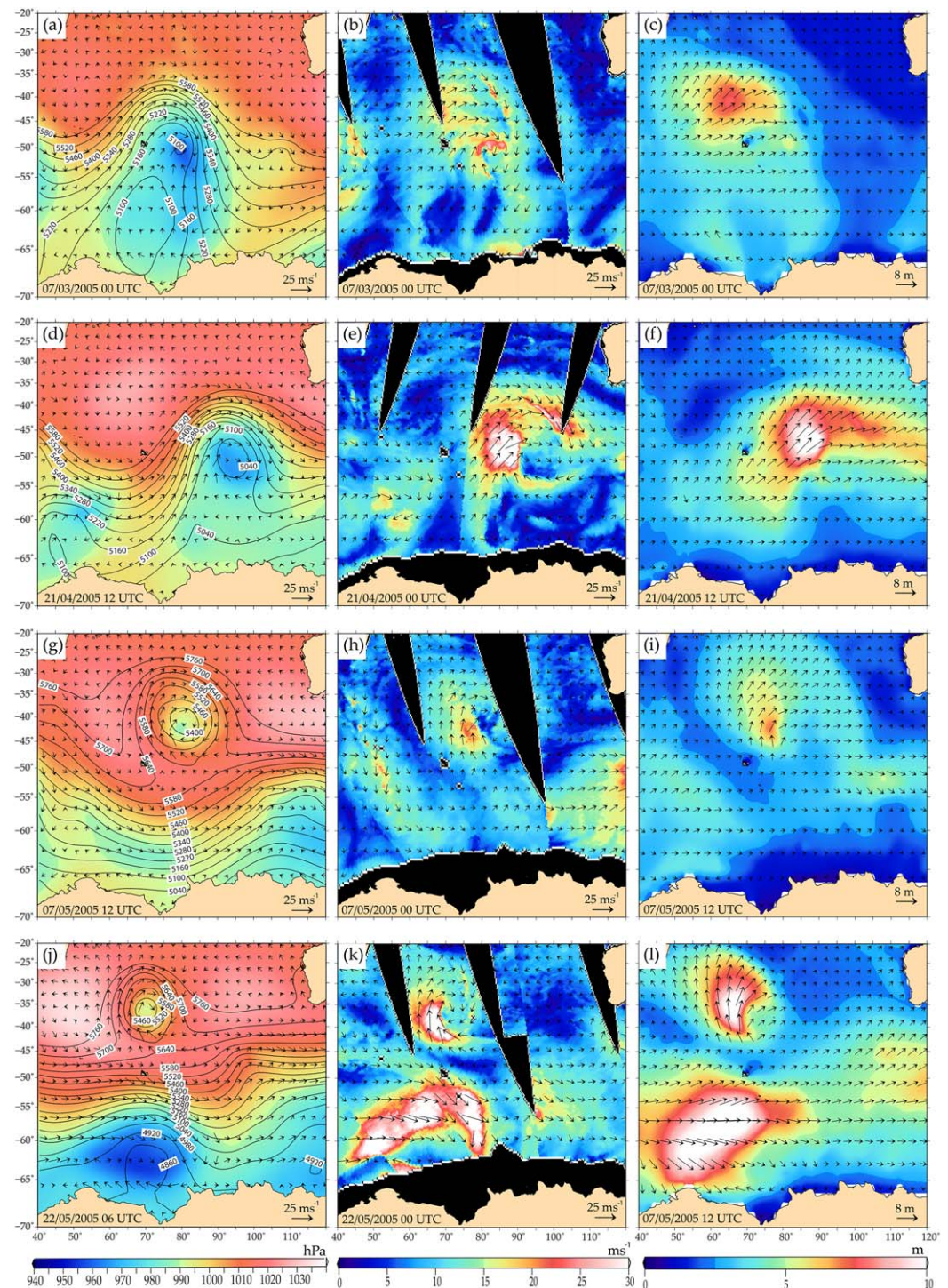


**Figure 10.** Maps showing four cases of Cut-Off Lows and associated wave propagation patterns observed during March–May 2005. (Left) Geopotential height at 500 hpa (contours; gpm), sea level pressure (shaded; hPa) and surface winds (vectors; m/s) are used to characterize the mature phase of Cut-Off Lows. (Middle) Surface winds (m/s) from QuikSCAT scatterometer. (Right) Wave propagation patterns associated with individual Cut-Off Low systems. Shades represent the magnitude and arrows show the direction of respective parameters in the middle and right panels.

COL with a stationary nature in the midlatitude (35°S–40°S) range can generate long-period swells, responsible for the high wave/Kallakkadal events along the Indian coastal region. Our results confirm that all the high energy low-frequency (0.04–0.055 Hz) swell bands reported from the buoys around India in 2005 are propagated from the SIO (60°S–30°S and 40°E–100° E) and are associated with COLs.

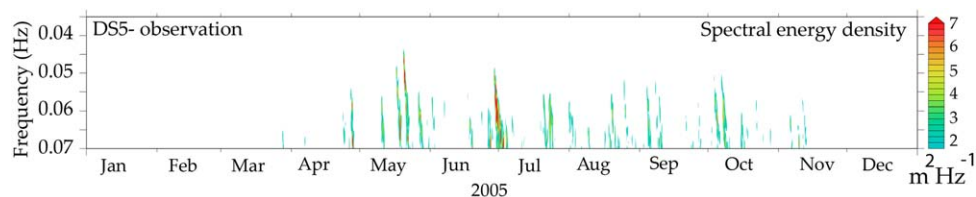


**Figure 11.** Evolution of wave energy density spectrum ( $\text{m}^2\text{Hz}^{-1}$ ) during 2005 at the deep sea mooring location, DS5, showing the high swell events.

### 6. Summary and Concluding Remarks

Coastal flooding is a serious issue as it poses threat to the life and property of the coastal population. If flooding occurs due to more predictable and locally visible weather features like cyclones or storm surges, then they can be predicted and damages can be averted to some extent. Along the south-west coast of India, unexpected coastal flooding has been reported many times which occur without any apparent reasons. Local people call this phenomenon as Kallakkadal, meaning the seas coming in as a thief and stealing their livelihoods. Ocean forecast systems, which usually look for local weather systems, generally fail to forecast these sorts of flooding events. In this article, we systematically analyzed the generation mechanism and environmental conditions that cause the flooding events along Indian coasts, using observations and numerical models.

Our analysis is limited to the observations from 2005, as we do not have adequate in situ data to ascertain the flooding episodes in other years. Detailed investigations with the buoy observations around India suggest that 10 number of high wave incidents occurred in 2005, all of which were driven by a surge in swell wave heights and not because of local winds. We have done a model sensitivity test in which we run the model with active winds only in the Southern Ocean. This simulation fully captured the swell conditions observed in the North Indian Ocean (NIO), ascertaining that all the 10 high swell conditions observed in 2005 were in fact driven by swells coming from the Southern Ocean. Among these high swell conditions, the 17–21 May 2005 event was very severe and caused Kallakkadal along Indian south-west coast. This motivated us to look into the atmospheric-ocean conditions in the Southern Ocean that led to the generation and propagation of swell waves into the NIO.

Many studies observed that the Cut-Off Low (COL) systems are very frequent in the Southern Ocean [Fuenzalida et al., 2005; Singleton and Reason, 2007]. COL systems are meteorological features developing as anomalous patterns in the westerly jet streams in the Southern Ocean. They can be identified in the weather charts as a closed geopotential height with a cold core. They are generally slow moving, often developed from the advection of cold air mass from the polar side toward equator and modulate the jet stream with a strong meridional component in the western side of the low pressure. While doing so, they provide the necessary conditions for the development of waves, i.e., strong and long duration winds over a large fetch. Our case study of the 17–21 May flooding event suggests that two very severe, and consecutive COL systems developed in the Southern Ocean during 12–17 May and were nearly stationary for 3 days in each case with

**Table 2.** Characteristic Details of South Indian Ocean Cut-Off Lows and the Associated Swell Events During 2005 Recorded at the DS5 Buoy

Date	Southern Ocean COL					Swell Events Off East Coast of India			
	Peak Intensity Location	BI	Duration (days)	Width (km)	U10 (m/s)	Date	Hs (m)	Tp (s)	Hss(m)
21-04-2005	47.2S 88.88E	4.25	1.25	880	28	2005-04-26	1.95	17.93	1.56
07-05-2005	39.4S 79.88E	3.51	6.25	2090	21	2005-05-10	2.03	17.93	1.48
14-05-2005	36S 90.00E	4.66	3.25	2420	28	2005-05-17	1.95	20.51	1.56
16-05-2005	38.2S 90.00E	4.17	3	1210	34	2005-05-20	1.95	22.26	1.71
22-05-2005	36S 68.62E	3.24	2.5	1760	26	2005-05-26	1.56	17.34	1.17
25-06-2005	54S 86.6E	4.97	5	1320	28	2005-06-29	3.67	18.28	2.3
17-07-2005	42.8S 77.63E	3.11	4.5	880	24	2005-07-21	2.03	18.28	1.17
28-09-2005	59.6S 90.00E	2.91	3.75	1100	30	2005-10-03	1.72	18.68	1.48
03-10-2005	37.1S 90.00E	3.33	2.75	880	26	2005-10-07	1.71	18.28	1.64

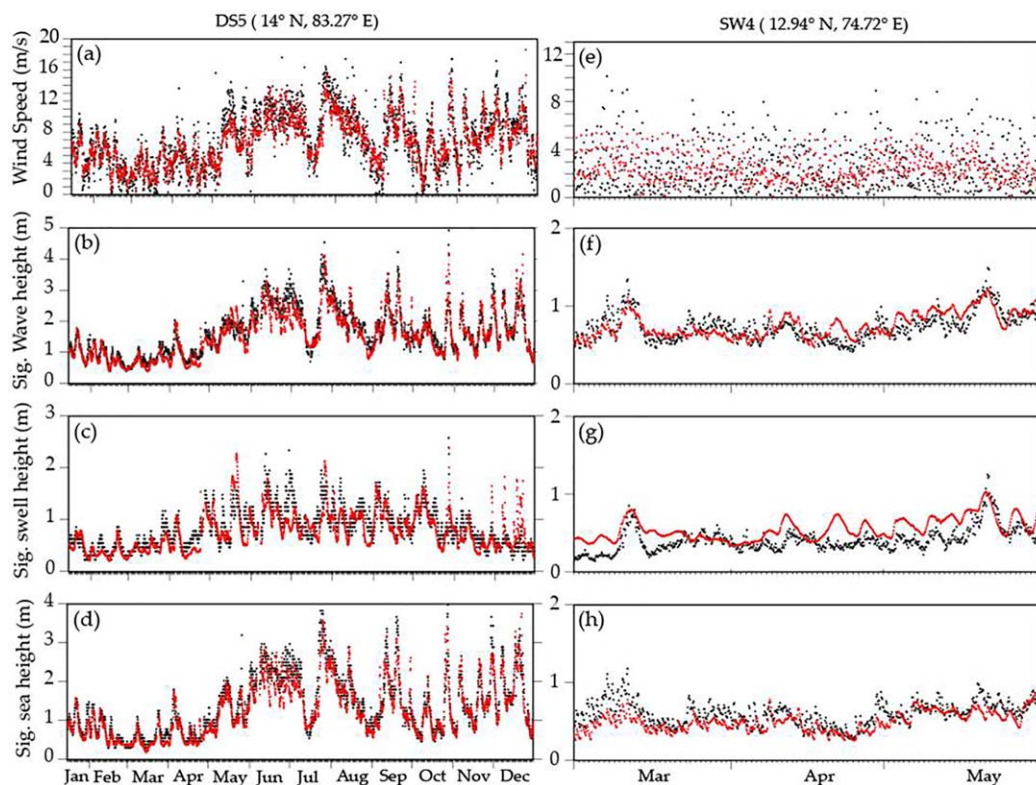


**Figure A1.** Comparison of model-derived wave parameters (red) with buoy-derived wave parameters (black) at DS5 and SW4 buoy locations.

maximum wind speed of more than  $\sim 25 \text{ ms}^{-1}$  over a large fetch. Wave simulations using WW3 confirm the generation of waves at the COL location and the propagation of swells into the NIO. The swell forerunners were typically of  $\sim 20$ s periods, and took  $\sim 4$  days to reach the NIO coastal regions. Thus swells coming from  $\sim 5700$  km down south created havoc in the coastal regions along south-west India during 17–21 May 2005.

Our NIO buoy observations recorded 10 high swell episodes in 2005, with periods generally more than 17 s, but not every case resulted in a large-scale coastal flooding, and hence went unnoticed. We looked at those high swell events using wave simulations and analyzed the meteorological conditions over SIO few days prior to the high swell events in the NIO. Origin of all such high swell incidents was associated with a COL system in the SIO 3–5 days before the high wave activity in NIO. These COLs are of high intensity with BI values more than 3. Location, intensity, duration, and quasistationary nature of the COLs determined the energy and period of the swell waves. Thus we conclude that the intense winds associated with the COLs in the SIO generate waves, and they travel to NIO as swells. Furthermore, these swells depending upon the local topography, angle of incidence, and tide conditions cause high wave activity along NIO coastal regions, and sometimes flooding along the coasts locally known as the Kallakkadal events.

The study of Fuenzalida *et al.* [2005] and Singleton and Reason [2007] shows that there is seasonality in the occurrence of COLs in the SIO. They are seen throughout the year with a maximum during March–May [Fuenzalida *et al.*, 2005]. The high swell events in our buoy observations are also seen in that period and hence our results are consistent with that of Fuenzalida *et al.* [2005]. One possible limitation of our study is that our inferences are drawn on the basis of analysis done for a single year. A multiyear modelling analysis would be ideal especially since long-time series in situ observations on wave parameters are nonextinct in the NIO.

Propagation of swells from the Southern Ocean and its interaction with local sea has been studied in the past [Nayak *et al.*, 2013]. A novel outcome of our analysis is a simple and relatively inexpensive approach to monitor and warn about the high wave events along NIO coasts. Our analysis suggests that proper monitoring of the oceanic-atmospheric conditions in the Southern Ocean from freely available forecast data sets should give a clue on the possible development of the COL events, and the subsequent generation and

**Table A1.** Model Error Statistics as Compared to Buoy Measurements

Buoy	Parameters	Bias	RMSE	SI	R
SW4 (NP = 1650)	Hs (m)	-0.06	0.18	0.19	0.93
	Hss (m)	0.03	0.13	0.27	0.86
	Hsb (m)	-0.09	0.20	0.25	0.96
	Tm (s)	1.37	1.56	0.30	0.75
	U <sub>10</sub> (ms <sup>-1</sup> )	-0.45	2.09	0.70	0.37
SW3 (NP = 1271)	Hs (m)	-0.25	0.30	0.28	0.98
	Hss (m)	-0.09	0.17	0.31	0.98
	Hsb (m)	-0.24	0.28	0.33	0.96
	Tm (s)	1.17	1.34	0.29	0.77
	U <sub>10</sub> (ms <sup>-1</sup> )	-2.59	3.58	0.67	0.64
SW5 (NP = 818)	Hs (m)	-0.20	0.25	0.34	0.71
	Hss (m)	-0.04	0.08	0.24	0.74
	Hsb (m)	-0.24	0.28	0.44	0.69
	Tm (s)	1.22	1.44	0.33	0.54
	U <sub>10</sub> (ms <sup>-1</sup> )	0.41	3.28	0.56	0.36
SW6 (NP = 1325)	Hs (m)	-0.06	0.19	0.24	0.76
	Hss (m)	-0.04	0.10	0.36	0.84
	Hsb (m)	-0.06	0.19	0.26	0.73
	Tm (s)	0.90	1.23	0.29	0.52
	U <sub>10</sub> (ms <sup>-1</sup> )	1.13	2.25	0.35	0.57
DS5 (NP = 2626)	Hs (m)	-0.21	0.36	0.21	0.92
	Hss (m)	-0.2	0.31	0.37	0.78
	Hsb (m)	-0.13	0.29	0.21	0.94
	Tm (s)	0.19	0.91	0.15	0.77
	U <sub>10</sub> (ms <sup>-1</sup> )	-0.30	1.78	0.25	0.87

propagation of swells into the Indian Ocean. The intensity and direction of the swells can be predicted and with the advance knowledge about the tidal conditions in the NIO, forecasters would be able to predict the high wave activity/Kallakkadal events in the NIO coastal regions at least 2–3 days in advance. An operational model set-up, as done for this analysis, but made in a real-time simulation mode would be ideal for such forecasting systems. This is a major focus of future research.

### Appendix A - Model Validation

A comparison of model-derived wave parameters (significant wave height (Hs), swell height (Hss), sea wave height (Hsb)) with buoy measured variables at the SW4 and DS5 location are shown in Figure A1. The comparison of wave heights (Hs, Hss, Hsb) at the deep water location shows fairly good agreement for the entire year considered. In the shallow water location, wave heights are quite low except high waves in a few isolated cases in the pre-monsoon period. Model simulated swell waves for the shallow water location shows overestimation in the low wave heights. Table A1 shows the model error statistics for wave parameters Hs, mean wave period (Tm), Hss, Hsb, and surface winds (U<sub>10</sub>). Various statistical measures like bias, root mean square error (RMSE), scatter index (SI), and correlation coefficient (R) are used to assess the model performance by comparing the model-derived parameters against the corresponding buoy measurements at SW3, SW4, SW5, SW6, and DS5 locations. Table A1 shows the model error statistics for wave parameters Hs, Tm, Hss, wind sea wave height (Hsb), and surface winds (U<sub>10</sub>). Model shows fairly good agreement with observation in all the locations. Among shallow water locations, a low value of scatter index for Hs (0.19) and Tm (0.3) is observed at the SW4 location. In the deep water location, model shows a very good agreement (SI <= 0.2 and R > 0.77) with buoy for both Hs and Tm.

### References

Alves, J. H. G. M. (2006), Numerical modelling of ocean swell contributions to the global wind-wave climate, *Ocean Modell.*, 11(1-2), 98–122

Andrade C. A., Y. F. Thomas, A. N. Lerma, P. Durand, and B. Anselme (2013), Coastal Flooding Hazard Related to Swell Events in Cartagena de Indias, Colombia, *J. Coastal Res.*, 290, 1126–1136.

Arduin, F., B. Chapron, and F. Collard (2009), Observation of swell dissipation across oceans, *Geophys. Res. Lett.*, 36, L06607, doi:10.1029/2008GL037030.

Arduin, F., et al. (2010), Semiempirical dissipation source functions for ocean waves. Part I: Definition, calibration, and validation, *J. Phys. Oceanogr.*, 40, 1917–1941.

Babanin, A. V. (2006), On a wave-induced turbulence and a wave-mixed upper ocean layer, *Geophys. Res. Lett.*, 33, L20605, doi:10.1029/2006GL027308.

### Acknowledgments

We thank Director, INCOIS, for encouraging us to carry out this work and facilitating the same. QuikSCAT data are produced by Remote Sensing Systems and sponsored by the NASA Ocean Vector Winds Science Team and can be obtained from www.remss.com. Era-Interim data are obtained from ECMWF from www.ecmwf.int/en/research/climate-reanalysis/era-interim. Blended Wind fields were obtained from the Centre de Recherche et d'Exploitation Satellitaire (CERSAT), at IFREMER, Plouzané (France). The in situ observations used for this study are obtained from www.incois.gov.in/portal/datainfo/mb.jsp. We thank the editor and two anonymous reviewers for the constructive comments on an earlier version of the manuscript which helped us to improve it. Finally, the financial support provided by the Earth System Science Organisation, Ministry of Earth Sciences, Government of India is gratefully acknowledged. This is INCOIS contribution 267.

- Barber, N. F., and F. Ursell (1948), The generation and propagation of ocean waves and swell. Part I. Wave periods and velocities, *Philos. Trans. R. Soc. London A*, *240*, 527–560.
- Bell, G. D., and L. F. Bossart (1989), A 15 year climatology of Northern Hemisphere 500 mb closed cyclone and anticyclone centre, *Mon. Weather Rev.*, *117*, 2142–2163.
- Bentamy, A., L. Ayina, P. Queffeuilou, D. Croize-Fillon, and V. Kerbaol (2007), Improved near real time surface wind resolution over the Mediterranean Sea, *Ocean Sci.*, *3*(2), 259–271.
- Chen, G., and S. E. Belcher (2000), Effects of long waves on wind-generated waves, *J. Phys. Oceanogr.*, *30*(9), 2246–2256.
- Collard, F., F. Ardhuin, and B. Chapron (2009), Routine monitoring and analysis of ocean swell fields using a space borne SAR, *J. Geophys. Res.*, *114*, C07023, doi:10.1029/2008JC005215.
- Dee, D. P., et al. (2011), The ERA-Interim reanalysis: Configuration and performance of the data assimilation system, *Q. J. R. Meteorol. Soc.*, *137*, 553–597, doi:10.1002/qj.828.
- Donelan, M. A. (1987), The effect of swell on the growth of wind waves, *Johns Hopkins APL Tech. Dig.*, *8*, 18–23.
- Fuenzalida, H., A. R. Sánchez, and R. D. Garreaud (2005), A climatology of cut-off lows in the Southern Hemisphere, *J. Geophys. Res.*, *110*, D18101, doi:10.1029/2005JD005934.
- Gimeno, L., R. M. Trigo, P. Ribera, and J. A. García (2007a), Special issue on cut-off low systems (COL), *Meteorol. Atmos. Phys.*, *96*, 1–2, doi:10.1007/s00703-006-0216-5.
- Grachev, A. A., and C. W. Fairall (2001), Upward momentum transfer in the marine boundary layer, *J. Phys. Oceanogr.*, *31*, 1698–1711.
- Grachev, A. A., C. W. Fairall, J. E. Hare, and J. B. Edson (2003), Wind stress vector over ocean waves, *J. Phys. Oceanogr.*, *33*, 2408–2429.
- Jones, T., M. Middelmann, and N. Corby (2005), Natural hazard risk in Perth, Western Australia, report, Geosci. Australia, Perth, ISBN:1 920871 43 8.
- Kurian, N. P., N. Nirupama, M. Baba, and K. V. Thomas (2009), Coastal flooding due to synoptic scale, meso-scale and remote forcings, *Nat. Hazards*, *48*, 259–273.
- Lupo, A. R., and P. J. Smith (1995a), Climatological features of blocking anticyclones in the Northern Hemisphere, *Tellus Ser. A*, *47*, 439–456.
- McInness, K. L., and G. D. Hubbert (2001), The impact of eastern Australian cut-off lows on coastal sea levels, *Meteorol. Appl.*, *8*, 229–244.
- Munk, W. H., and F. E. Snodgrass (1957), Measurement of Southern Ocean swell at Guadalupe island, *Deep Sea Res.*, *4*, 272–286.
- Munk, W. H., G. R. Miller, F. E. Snodgrass, and N. F. Barber (1963), Directional recording of swell from distant storms, *Philos. Trans. R. Soc. London A*, *255*, 505–584.
- Nayak, S., P. K. Bhaskaran, R. Venkatesan, and S. Dasgupta (2013), Modulation of local wind-waves at Kalpakkam from remote forcing effects of Southern Ocean swells, *Ocean Eng.*, *64*, 23–35.
- Nieto, R., M. Sprenger, H. Wernli, R. M. Trigo, and L. Gimeno (2008), Identification and climatology of cut-off low near the tropopause, *Ann. N. Y. Acad. Sci.*, *1146*, 256–290, doi:10.1196/annals.1446.016.
- Reboita, M. S., R. Nieto, L. Gimeno, L. R. P. da Rocha, T. Ambrizzi, R. Garreaud, and L. F. Kruger (2010), Climatological features of cut-off low systems in the Southern Hemisphere, *J. Geophys. Res.*, *115*, D17104, doi:10.1029/2009JD013251.
- Remya, P. G., R. Kumar, S. Basu, and A. Sarkar (2012), Wave hindcast experiments in the Indian Ocean using MIKE 21 SW model, *J. Earth Syst. Sci.*, *121*, 385–392.
- Sabique, L., K. Annapurnaiah, T. M. Balakrishnan Nair, and K. Srinivas (2012), Contribution of Southern Indian Ocean swells on the wave heights in the Northern Indian Ocean: A modeling study, *Ocean Eng.*, *43*, 113–120.
- Sandhya, K. G., P. G. Remya, T. M. Balakrishnan Nair, and N. Arun (2015), On the co-existence of high-energy low-frequency waves and locally-generated cyclone waves off the Indian east coast, *Ocean Eng.*, *111*, 148–154.
- Shyu, J. H., and O. M. Phillips (1990), The blockage of gravity and capillary waves by longer waves and currents, *J. Fluid Mech.*, *217*, 115–141.
- Silbey A, and D. Cox (2015), Coastal flooding in England and Wales from Atlantic and North Sea storms during the 2013/2014, *Weather*, *70*(2), 62–70.
- Singleton, A. T., and C. J. C. Reason (2007), Variability in the characteristics of cut-off low pressure systems over subtropical southern Africa, *Int. J. Climatol.*, *27*, 295–310.
- Smedman, A. S., X. G. Larsen, U. Hogstrom, K. K. Kahma, and H. Pettersson (2003), Effect of sea state on the momentum exchange over the sea during neutral conditions, *J. Geophys. Res.*, *108*(C11), 3367, doi:10.1029/2002JC001.
- Snodgrass, F. E., G. W. Groves, K. Hasselmann, G. R. Miller, W. H. Munk, and W. H. Powers (1966), Propagation of ocean swell across the Pacific, *Philos. Trans. R. Soc. London A*, *249*, 431–497.
- Tolman, H. L., and the WAVEWATCH III<sup>®</sup> Development Group (2014), *User Manual and System Documentation of WAVEWATCH III<sup>®</sup> version 4.18*, Tech. Note 316, NOAA/NWS/NCEP/MMAB, 282 pp.+ Appendices, University Research Court College Park, Md.
- Tracy, B., J. Hanson, E. Devaliere, S. Nicholini, and H. Tolman (2007), Wind seas and swell delineation for numerical wave modeling, paper presented at 10th International Workshop on Wave Hindcasting and Forecasting and Coastal Hazard Symposium, Coastal and Hydraul. Lab., Eng. Res. and Dev. Cent., U.S. Army Corps of Eng., North Shore, Oahu, Hawaii, 11–16 Nov.
- Wiedenmann, J. M., A. R. Lupo, Mokhov II, and E. A. Tikhonova (2002), The climatology of blocking anticyclones for the Northern and Southern Hemisphere block intensity as a diagnostic, *J. Clim.*, *15*, 3459–3473.
- Young, I. R., A. Babanin, and S. Zieger, (2013), The decay rate of ocean swell observed by altimeter, *J. Phys. Oceanogr.*, *43*, 2322–2333.